

## Erratum: High-temperature superconductivity in atomic metallic hydrogen [Phys. Rev. B **84**, 144515 (2011)]

Jeffrey M. McMahon\* and David M. Ceperley†

(Received 26 May 2012; published 19 June 2012)

DOI: [10.1103/PhysRevB.85.219902](https://doi.org/10.1103/PhysRevB.85.219902)

PACS number(s): 74.20.Pq, 74.10.+v, 74.62.Fj, 74.20.Fg, 99.10.Cd

In Ref. 1, herein referred to as *I*, labels designating the crystal structures under consideration were omitted from some figures, which could be a source of confusion. Moreover, superconducting parameters necessary to estimate critical temperatures,  $T_c$ , were calculated using the nonweighted phonon density of states,  $F(\omega)$ , rather than the proper normalized weighting function of the Eliashberg theory,<sup>2</sup>  $g(\omega)$ .

In this Erratum, we first review the theoretical background for calculating the parameters needed to estimate  $T_c$ , in particular their evaluation using  $g(\omega)$ . We then present and discuss results analogous to Figs. 4, 5, and 13 of *I* with revised calculations and including crystal-structure labels. Finally, we provide a brief summary of the differences between calculations.

In order to evaluate the McMillan formula<sup>2,3</sup> or the Allen-Dynes equation<sup>4</sup> to estimate  $T_c$ , Eqs. (2) and (3) of *I*, respectively, we must determine  $\lambda$ ,  $\langle\omega\rangle$ ,  $\bar{\omega}_2$ ,  $\omega_{\ln}$ , and  $\mu^*$ ; these correspond to the attractive electron-phonon-induced interaction, the first and square root of the second moments of  $g(\omega)$ , the logarithmic average phonon frequency [i.e.,  $\ln(\omega_{\ln}) = \langle\ln\omega\rangle$ ], and the renormalized Coulomb repulsion, respectively. As in *I*, below we take the approximate, yet reasonable,<sup>5</sup> value of 0.089 for  $\mu^*$ . Further,  $\lambda$  is a direct measure of the strength of the electron-phonon spectral function  $\alpha^2F(\omega)$ , which is readily calculable via *ab initio* calculations,<sup>6</sup>

$$\lambda = 2 \int_0^\infty d\omega \alpha^2 F(\omega) / \omega. \quad (1)$$

$\langle\omega\rangle$ ,  $\bar{\omega}_2$ , and  $\omega_{\ln}$  can also be calculated directly from  $\alpha^2F(\omega)$ ,

$$\langle\omega\rangle = \int_0^\infty d\omega g(\omega) \omega, \quad (2)$$

$$\bar{\omega}_2 = \left[ \int_0^\infty d\omega g(\omega) \omega^2 \right]^{1/2}, \quad (3)$$

$$\omega_{\ln} = \exp \left[ \int_0^\infty d\omega g(\omega) \ln(\omega) \right], \quad (4)$$

where

$$g(\omega) = \frac{2}{\lambda\omega} \alpha^2 F(\omega). \quad (5)$$

The difference between Eqs. (2)–(4) and those presented and used in *I* is via the use of  $g(\omega)$  in place of  $F(\omega)$ , which results in weighted averages.  $\lambda$ ,  $\langle\omega\rangle$ , and  $\omega_{\ln}$  calculated using Eqs. (1), (2), and (4), as well the corresponding estimates of  $T_c$  calculated using Eqs. (2) and (3) of *I*, are presented and discussed below.

$\lambda$ . The use of  $g(\omega)$  in Eqs. (2)–(4) does not affect the calculation of  $\lambda$ . Nonetheless, in Fig. 1, we show again  $\lambda$  values for both the  $I4_1/amd$  and  $R-3m$  structures<sup>7</sup> considered in *I*, but we now include crystal-structure labels.

Note that values for  $R-3m$  are not shown between  $\sim 1$  and 2 TPa (as in *I*), because of complications in applying Eqs. (2)–(4) in the presence of (unphysical) imaginary phonon frequencies (see below).

$\langle\omega\rangle$  and  $\omega_{\ln}$ . Temperature prefactors  $\langle\omega\rangle/k_B$  and  $\omega_{\ln}/k_B$ , where  $k_B$  is Boltzmann's constant, calculated using Eqs. (2)–(4), including crystal-structure labels, are shown in Fig. 2.

As in *I*,  $\langle\omega\rangle$  and  $\omega_{\ln}$  both exhibit similar trends with pressure, the latter at a slightly lower magnitude. Further, when  $g(\omega)$  is used in Eqs. (2) and (4) instead of  $F(\omega)$ , there is a decrease in the magnitudes of both (compare, for example, directly with Fig. 4 of *I*). At relatively low pressure, there is only a minor difference (e.g., the prefactors are  $\sim 2000$  K near 500 GPa, as opposed to  $\sim 2200$  K). As the pressure is increased, however, which causes the phonon frequencies to move correspondingly higher, the difference becomes greater (e.g., at 3 TPa, the prefactors become  $\sim 2250$  K, as opposed to 3600 K). This latter result suggests that the corresponding  $T_c$  values will be somewhat reduced as well (see below).

We note that values are not shown for pressures near 1–2 TPa for  $R-3m$ . This is a consequence of the (classically predicted) instabilities in this pressure range.<sup>1,7</sup> For a classically unstable structure, imaginary phonon frequencies can appear in the phonon dispersion. Because of this,  $\alpha^2F(\omega)$  becomes finite as  $\omega \rightarrow 0$ , and this causes an unbound and unphysical increase in  $g(\omega)$  (see also Figs. 10 and 11 of *I*).

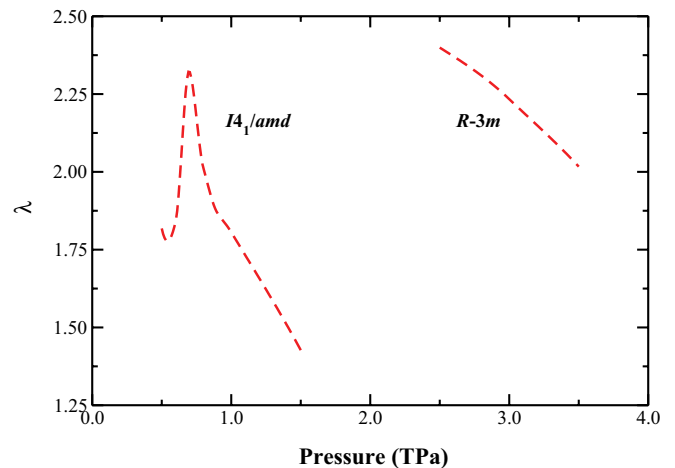


FIG. 1. (Color online) Electron-phonon-induced interaction,  $\lambda$ , as a function of pressure.

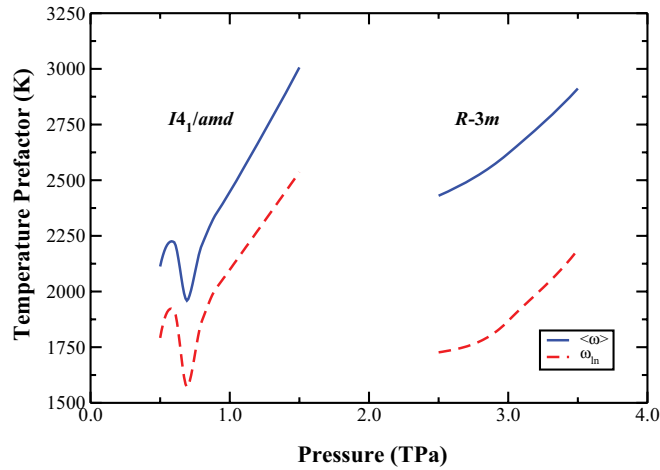


FIG. 2. (Color online) Temperature prefactors  $\langle\omega\rangle/k_B$  (solid blue line) and  $\omega_{\text{in}}/k_B$  (dashed red line) as a function of pressure.

Equations (2)–(4), under such circumstances, cannot therefore be reliably evaluated.

$T_c$ . Estimated  $T_c$  values calculated using the weighted superconductivity parameters in Eqs. (2)–(4), including crystal-structure labels, are shown in Fig. 3.

As expected, the estimated  $T_c$  values are somewhat reduced compared to those in *I*. Nonetheless, the qualitative physics remains the same. Near molecular dissociation ( $\sim 500$  GPa), superconductivity is still predicted to occur above room temperature. As the pressure is increased and the atomic phase stabilizes,  $T_c$  increases. However, in contrast to the results reported in *I*,  $T_c$  is predicted to only reach  $\sim 360$  K, as opposed to 481 K. Further, at the atomic-atomic structural phase transformation ( $I4_1/amd \rightarrow R-3m$ ),  $T_c$  is still expected to increase. While we cannot reliably estimate  $T_c$  precisely near 1–2 TPa, as discussed above, we can infer this based on

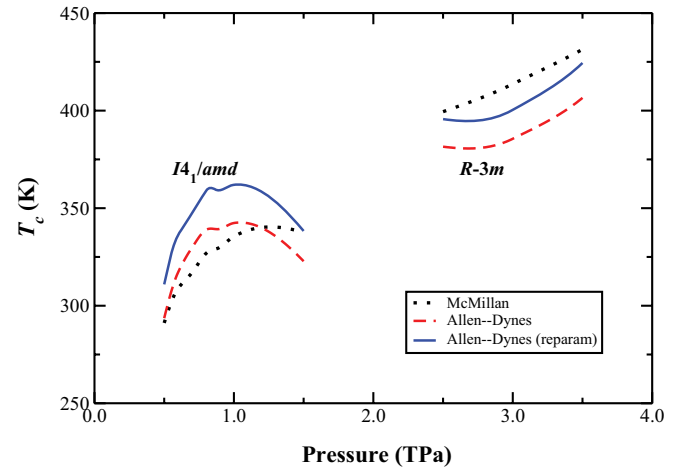


FIG. 3. (Color online) Superconducting critical temperatures,  $T_c$ , calculated using Eqs. (2) and (3) of *I*, as a function of pressure.

the large  $T_c$  values at higher pressure (e.g., near 3 TPa,  $T_c$  approaches 425 K).

In conclusion, we presented results to replace Figs. 4, 5, and 13 of *I*. The new figures contain crystal-structure labels to prevent possible confusion, as well as revised and more reliable (properly calculated) values of  $\langle\omega\rangle$ ,  $\omega_{\text{in}}$ , and  $T_c$ . While some differences in results exist relative to those reported in *I*, their qualitative features remain unchanged. In particular,  $T_c$  values (Fig. 3) remain remarkably high, above room temperature, which continues to suggest the interesting possibility that the atomic phase of hydrogen exists entirely in a superconducting state.

We thank N. W. Ashcroft for pointing out the lack of crystal-structure labels in some figures of *I*.

\*mcmahonj@illinois.edu

†ceperley@ncsa.uiuc.edu

<sup>1</sup>J. M. McMahon and D. M. Ceperley, *Phys. Rev. B* **84**, 144515 (2011).

<sup>2</sup>W. L. McMillan, *Phys. Rev.* **167**, 331 (1968).

<sup>3</sup>R. C. Dynes, *Solid State Commun.* **10**, 615 (1972).

<sup>4</sup>P. B. Allen and R. C. Dynes, *Phys. Rev. B* **12**, 905 (1975).

<sup>5</sup>C. F. Richardson and N. W. Ashcroft, *Phys. Rev. Lett.* **78**, 118 (1997).

<sup>6</sup>M. Wierzbowska, S. de Gironcoli, and P. Giannozzi, *arXiv:cond-mat/0504077*.

<sup>7</sup>J. M. McMahon and D. M. Ceperley, *Phys. Rev. Lett.* **106**, 165302 (2011).